Snow Depth on Arctic Sea Ice

STEPHEN G. WARREN, IGNATIUS G. RIGOR, AND NORBERT UNTERSTEINER

Department of Atmospheric Sciences, University of Washington, Seattle, Washington

VLADIMIR F. RADIONOV, NIKOLAY N. BRYAZGIN, AND YEVGENIY I. ALEKSANDROV

Arctic and Antarctic Research Institute, St. Petersburg, Russia

ROGER COLONY

International Arctic Research Center, University of Alaska, Fairbanks, Alaska

(Manuscript received 5 December 1997, in final form 27 July 1998)

ABSTRACT

Snow depth and density were measured at Soviet drifting stations on multiyear Arctic sea ice. Measurements were made daily at fixed stakes at the weather station and once- or thrice-monthly at 10-m intervals on a line beginning about 500 m from the station buildings and extending outward an additional 500 or 1000 m. There were 31 stations, with lifetimes of 1–7 yr. Analyses are performed here for the 37 years 1954–91, during which time at least one station was always reporting.

Snow depth at the stakes was sometimes higher than on the lines, and sometimes lower, but no systematic trend of snow depth was detected as a function of distance from the station along the 1000-m lines that would indicate an influence of the station. To determine the seasonal progression of snow depth for each year at each station, priority was given to snow lines if available; otherwise the fixed stakes were used, with an offset applied if necessary.

The ice is mostly free of snow during August. Snow accumulates rapidly in September and October, moderately in November, very slowly in December and January, then moderately again from February to May. This pattern is exaggerated in the Greenland–Ellesmere sector, which shows almost no net accumulation from November to March. The Chukchi region shows a steadier accumulation throughout the autumn, winter, and spring. The average snow depth of the multiyear ice region reaches a maximum of 34 cm (11 g cm^{-2}) in May. The deepest snow is just north of Greenland and Ellesmere Island, peaking in early June at more than 40 cm, when the snow is already melting north of Siberia and Alaska. The average snow density increases with time throughout the snow accumulation season, averaging 300 kg m^{-3}, with little geographical variation.

Usually only two stations were in operation in any particular year, so there is insufficient information to obtain the geographical pattern of interannual variations. Therefore, to represent the geographical and seasonal variation of snow depth, a two-dimensional quadratic function is fitted to all data for a particular month, irrespective of year.

Interannual anomalies for each month of each year are obtained relative to the long-term mean snow depth for the geographical location of the station operating in that particular year. The computed interannual variability (IAV) of snow depth in May is 6 cm, but this is larger than the true IAV because of inadequate geographical sampling. Weak negative trends of snow depth are found for all months. The largest trend is for May, the month of maximum snow depth, a decrease of 8 cm over 37 yr, apparently due to a reduction in accumulation-season snowfall.

1. Introduction

The surface waters of the Arctic Ocean and its marginal seas freeze to form a layer of sea ice up to a few meters in thickness. At the end of winter the ice covers an area of 14×10^6 km^2 [Fig. 3.1.45 of Gloersen et al. (1992)]. In summer the ice melts completely over about half of this area, leaving a residual 7×10^6 km^2 of multiyear sea ice, restricted to the central Arctic Ocean, that survives through the summer. Snowfall accumulates on the sea ice during autumn, winter, and spring. The snow melts rapidly in early summer, leaving puddles on the ice in many places, and the bare ice subsequently undergoes further melting at its upper and lower surfaces during the summer.

The snow has several important effects on the climate of the sea-ice region. The large air content of snow

Corresponding author address: Stephen G. Warren, Department of Atmospheric Sciences, Box 351640, Seattle, WA 98195.
E-mail: sgw@atmos.washington.edu

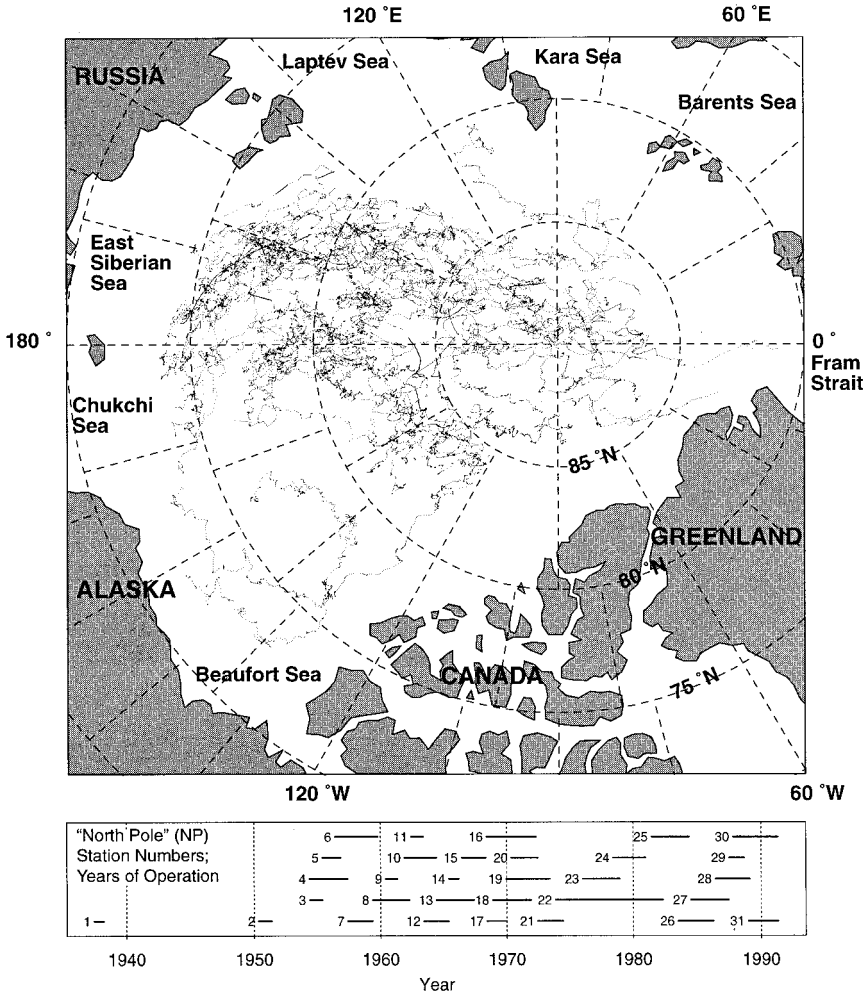

FIG. 1. Paths of NP drifting stations NP-3 through NP-31. Lower frame shows years of operation of each drifting station.

causes it to be a poor conductor of heat (Sturm et al. 1997, 1998) and also causes solar photons to undergo numerous scattering events so that penetration of light is impeded, resulting in a high albedo (Grenfell and Maykut 1977). The insulating effect of snow reduces the rate at which seawater freezes to the bottom of the ice, whereas the high albedo of snow reduces the rate of ice melting at the top in summer; the resulting dependence of ice thickness and salinity profiles on the snow thickness is therefore complex (Maykut and Untersteiner 1971; Ledley 1991). When the snow melts, it becomes an input of freshwater that affects the salinity and density structure of the ocean. For all these reasons, a climatology of snow accumulation, including its geographical, seasonal, and interannual variations, is needed for climatic analyses and climate modeling.

Many manned stations have been established on the drifting multiyear ice of the central Arctic to carry out oceanographic and atmospheric measurements. The largest program, by far, was the series of 31 ''North Pole'' (NP) drifting stations operated by the Soviet Union, begun in 1937 and providing continuous coverage from 1954 to 1991. This paper presents an analysis of the snow depth measurements at those stations. We also compare the results to the earlier climatologies that were limited in space and time: a seasonal cycle for 1 yr at U.S. Drifting Station A (Untersteiner 1961) and an analysis of the first nine NP stations (Loshchilov 1964).

2. Method of analysis

a. Data available

Figure 1 shows the tracks of the NP drifting stations 3–31 during the years 1954–91. The data collected at these stations are limited to the region of multiyear ice. Beginning in 1954 there was always at least one operating station, usually two, and occasionally three, at any one time (lower panel of Fig. 1). Most of the stations

FIG. 2. Photographs at station NP-6. (a) Measuring distance along a snow line. (b) Weighing snow to obtain its density. (Photographs by N. N. Bryazgin, 1957.)

were established on multiyear sea ice; five of them were on ice islands (Crary 1956).

Snow depth was measured in two ways at the NP stations. A set of three stakes spaced 25 m apart at three corners of the weather station, not far from the station buildings, was measured daily. Snow depth was also measured at 10-m intervals on a line beginning at least 500 m from the station and extending outward another 500 or 1000 m (Fig. 2a). Two-thirds of the snow lines were 500 m long; one-third were 1000 m. Snow density (the average density of a vertical column) was measured every 100 m along the line by weighing a cylinder that had been pushed vertically down to the snow–ice interface (Fig. 2b). The direction of the snow line was chosen randomly when a station was established, but once chosen, subsequent measurements were made along that same line for the lifetime of the station. The snow lines were measured once or thrice per month at each station; a total of 499 measurements during the years 1954–91. The snow line was marked by permanent stakes only at its ends; there were no stakes at the 10-m intervals. Some disturbance of the snow was caused by walking along the snow line; therefore, each successive monthly or 10-day snow line was offset about

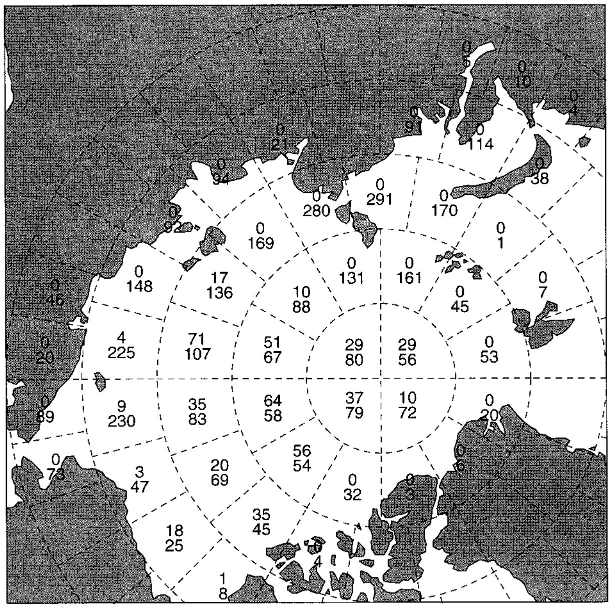

FIG. 3. Number of snow lines measured at North Pole drifting stations (upper number in each grid box), and number of Sever airplane landings providing snow depth reports in spring (lower number).

3 m from, but parallel to, the previous one. Measurements were made on a snow line only when the snow depth exceeded 5 cm and at least 50% of the area was covered. In the remainder of this paper we will use ''snow line'' or ''snow line measurement'' to mean the entire sequence of 50 or 100 snow depth readings along a snow line.

A complete description of the snow measurements at the NP stations is given by Radionov et al. (1996). The snow depth and snow density data, as well as meteorological data from these stations, are now available on electronic media from the National Snow and Ice Data Center (www-nsidc.colorado.edu); this dataset is described by Colony et al. (1998). Radiosonde data from these stations have also been archived, augmenting the dataset described by Kahl et al. (1992).

When available, we use measurements on the snow lines in preference to those at the stakes, for two reasons: 1) The snow lines cover a long enough track to obtain a representative distribution of snow depths, passing through sastrugi, snow dunes, and pressure ridges as well as level snow. 2) Drifting of snow around the station, and reduced albedo due to station activities, can make the stake measurements unrepresentative of the surrounding area.

Measurements of snow depth were also made during the *Sever* program of airplane landings (Romanov 1996). (Sever is the Russian word for north.) This program was carried out from 1959 to 1988, only in spring; most of the measurements were made in April. Landings were made not only on the multiyear ice but also on seasonal sea ice along the Siberian coast in regions not sampled by the drifting NP stations. Snow depth is given by Romanov not as an areal average but instead separately for each of four categories of snow: snow on prevailing ice of the landing area, sastrugi, drifts behind ridges, and average of windward and leeward sides of hummocks.

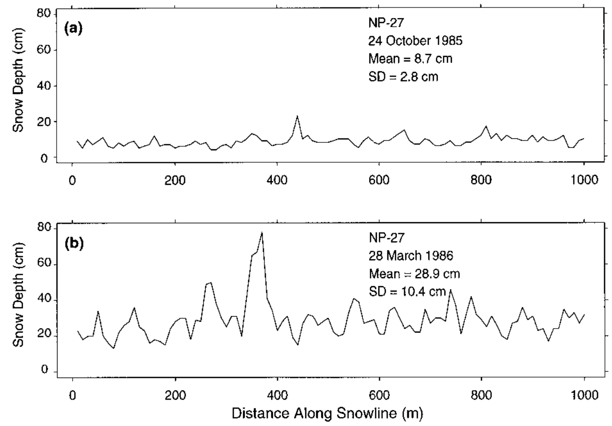

FIG. 4. Snow depth measured at 10-m intervals along two snow lines at station NP-27. (a) In autumn, early in the accumulation season. (b) In spring. Here SD means standard deviation.

Figure 3 shows the geographical distribution of NP snow line measurements and Sever aircraft landings.

b. Sampling statistics

Examples of snow line measurements are shown in Fig. 4 for 2 months: October, with thin snow cover early in the accumulation season, and March, with deeper snow. For both snow lines the number of measurements is $N = 100$, spaced at 10-m intervals. The spatial variability increases as the winter progresses; on both snow lines the standard deviation (SD) of snow depth is about one-third of the mean. The deep snow at about one-third of the way along the line in March is probably in a snow dune or in a drift near a pressure ridge.

If we assume that successive 10-m values are independent measurements (this assumption is justified below), we can estimate the uncertainty of mean snow depth as SD/$N^{1/2}$, which is 0.3 cm in October and 1.0 cm in March for this particular station. Somewhat larger estimates are obtained by the following method, which uses data from several 1000-m snow lines. A subset of size N_s is drawn at random from the 100 snow depth values on an individual snow line, and their depths are averaged. The difference between this average and the average of the complete set is the error due to inadequate sampling. The experiment is repeated 20 times for the same value of N_s, and the root-mean-square (rms) error ε is obtained for that value of N_s for that snow line. The rms error is plotted in Fig. 5 as a function of the size of the subset N_s. Because the subsets are compared to the mean of $N = 100$ points rather than to the true mean of an infinite number of points, ε drops artificially to zero at $N_s = N$, but lines of slope -0.5 adequately fit

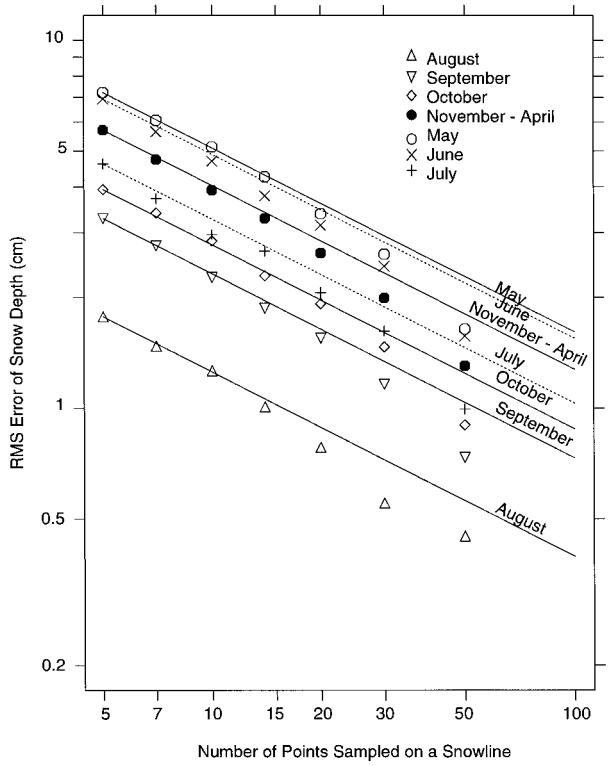

FIG. 5. Expected error in the mean of a set of snow depth measurements, as a function of the number of measurements used to compute the mean. Subsets of 5–50 points on a snow line were selected randomly from the complete set of 100 points; the error is defined as the difference between the mean of the subset and the mean of the complete set. This was done for several 1000-m snow lines at several NP stations; their averages are plotted here.

the first few points, indicating that the depth measurements spaced 10 m apart are independent. We therefore estimate the expected error for $N_s = 100$ by assuming $\varepsilon \sim N_s^{-1/2}$ and fitting lines of this slope to the values of ε for small N_s ($N_s \leq 15$). Extrapolation of these lines indicates that the uncertainty in mean snow depth for a single 100-point snow line is 1.3 cm through the winter (November–April). It is smaller in autumn and peaks at 1.6 cm in May, the month of deepest snow. For a 50-point snow line the corresponding uncertainties are 1.8 cm in winter and 2.3 cm in May.

c. *Influence of the station*

Drifting of snow around station buildings can cause deviations from the natural snow accumulation patterns. If the snow lines are affected, we would expect to find a systematic decrease of snow depth with distance from the station. To search for such a trend, we formed 10-point (100-m) averages for each 500-m and 1000-m snow line and examined the 499 plots of 5 or 10 points each (one for each snow line). No significant trends were found that persisted from 1 month to the next. Averaging all snow lines of each NP station point-by-point also

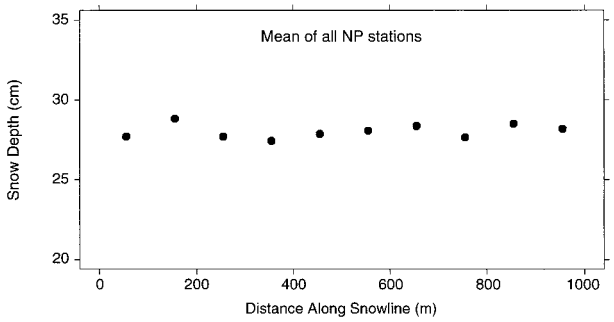

FIG. 6. Snow depth as a function of distance along a snow line, average of all 1000-m snow lines at all NP stations, and averaged over 100-m intervals. Each snow line starts several hundred meters from the station buildings and continues from this zero point directly outward for 1000 m.

failed to provide evidence for an influence of the station; nor does the grand average of all stations (Fig. 6). We conclude that the starting points of snow lines were far enough from the station buildings to escape their influence on wind drifting. This is also to be expected, because the buildings at the NP stations were mostly small, no higher than many of the pressure ridges.

d. *Snow stakes versus snow lines*

Snow depth measurements at stakes are available for some months when snow lines were not measured, so we would like to use them if they can be a reliable proxy for the missing snow line data. Figure 7 compares the average snow depth on each snow line with the depth at the stakes

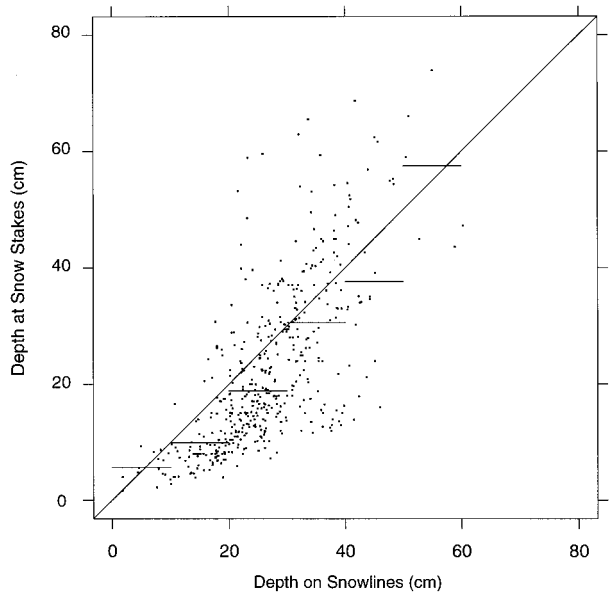

FIG. 7. Average snow depth on each snow line, compared to average snow depth at stakes at the weather station on the 5 days surrounding the day that the snow line was measured. Horizontal bars are averages of all points in 10-cm bins of snow line depth.

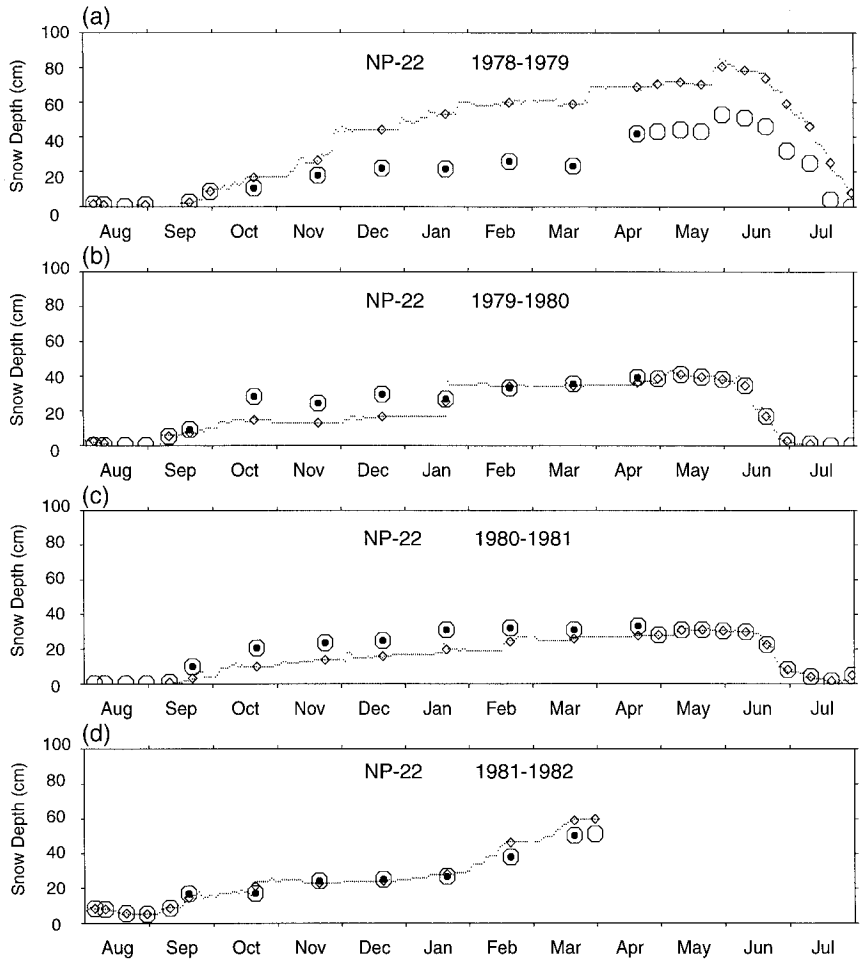

FIG. 8. Selection of data to be used for snow depth climatology. The example shown is the last 4 yr of station NP-22. Large solid dots are means of individual monthly snow lines. Small dots are means of three stakes measured daily. Open diamonds are 5-day means of stake values, centered on the time of the snow line measurement. Large open octagons are our choices of data to be used. Values at 5-day intervals are then obtained by interpolating between the choices in months when the choices are more than 5 days apart.

on the 5 days surrounding the day that the line was measured. There is more scatter in the stake values because each is an average of only 15 points, whereas each snow line value is an average of 50 or 100 points. To look for an overall bias, groups of stake data in Fig. 7 were averaged within 10-cm bins of depth as measured on the lines. These averages, shown as the horizontal bars in Fig. 7, show a tendency to be biased low by a few centimeters, but the difference is small enough that we have decided to use stake data when needed, with an offset applied if necessary as discussed below.

e. Data selection

The seasonal progression of snow depth was examined individually for each NP station in each year of operation, considering both stake data and snow line data. From these data, which are available at somewhat irregular intervals and with some gaps, especially over summer, we constructed an estimate of the snow depth at 5-day intervals throughout the operating life of the station, which was usually 2–3 yr. Priority was given to snow line data if available. Figure 8 illustrates the procedure, using the example of the station NP-22, in operation from 1974 to 1982. The figure shows only the last 4 yr of its operation. Large solid dots indicate the snow line measurements, which were made monthly at this station, usually on the 20th of each month. The daily snow stake data are shown as small dots; 5-day means of the stakes, centered on the day of the snow line measurement, are shown as the diamonds. The difference between the last simultaneous snow stake and snow line values is used as an indication of whether an offset needs to be applied when snow line data terminate and we have to make a connection to the continuing stake record.

Our choices of data values are indicated by the large octagons; we then interpolate between them at 5-day intervals to create a dataset that is uniformly sampled in time, to be used for the climatological analyses below. Our ''snow depth year'' begins on 1 August. Our rationale for the choices in Fig. 8 is as follows. Every snow line is a choice; these are always our preferred data. They begin in September or October of each of these 4 yr. We use data from the stakes in August and September 1978, then transition to the October snow line. Snow lines are chosen through the winter and spring of 1979 until they terminate in April. In this year there was a huge difference between snow depth at the stakes and snow depth on the lines (that is why we chose this year for illustration; cf. Fig. 7). The stakes were apparently located in a drift. We determine the offset in April as 28 cm but reduce this offset somewhat as the snow melts. We subtract the offset from the stake data of May, June, and July, to obtain the values indicated by the large open octagons. These octagons are our estimate of what the snow line would have recorded had it been measured.

A small amount of snow was recorded at the stakes in early August 1979, dropping to zero on 10 August, after which there are no measurements for the next month because of an absence of snow. We therefore insert zeros into the dataset until the stake record resumes in September. A transition is made from the stakes on 10 September to the first snow line on 20 September. Snow lines are chosen until 20 April 1980, the last measurement before the summer break. Because the stakes are in good agreement with the lines for the previous 2 months, our choice subsequently follows the stakes from late April through the rapid snowmelt until the snow disappears in early July. Zeros are inserted through the summer until the record begins again in September.

The 1980–81 accumulation year was processed in a manner similar to the preceding year. The following summer of 1981 was unusual in that sufficient snow fell during summer that there was always some snow at the stakes. At the end of the record, in February and March 1982, the snow stakes are biased high. Therefore, after the last snow line on 20 March we apply an offset to the subsequent stake data.

The station was decommissioned in April 1982. For some NP stations the record of snow depth continues through the melt in June but does not resume in the autumn. In those cases we cannot assume that a lack of measurements in the summer means no snow. We therefore insert zeros through the summer only if the record resumes at the same station in autumn.

3. Snow cover climatology

With reference to Fig. 3, it would be desirable to describe the seasonal cycle and interannual variations of snow depth in each of the 18 grid boxes occupied by the drifting stations. Such a complete description would require about 8000 snow lines total (18 boxes $\times$ 37 yr $\times$ 12 months). Since typically only two drifting stations were operating at any time, such a complete climatic description is not possible. A total of only 499 snow lines were measured. When the augmentation of the record by snow stakes is considered, as well as the inferred zeros in summer, we have the equivalent of about 800 snow lines. This is sufficient to obtain (a) the multiyear average seasonal and geographical variation and (b) the interannual variations of the Arctic mean snow depth, but not (c) the geographical pattern of interannual variations.

a. Geographical variation of snow depth

To obtain the average geographical pattern of snow depth for a month, we use all measurements from all NP stations made in that month, irrespective of year. In a single year there are usually only two stations reporting, but by using data from all 37 yr, we obtain good geographical coverage across the central Arctic in each month. A two-dimensional quadratic function with six unknown coefficients, defined in Table 1, is fitted by a least squares procedure to the values of snow depth produced by the method described in section 2e. The six 5-day values in a month are averaged to obtain a single value representative of midmonth at each station. There were on average two stations reporting in each of 37 yr, so the number of independent data values is about 70, which is sufficient for a robust determination of the six coefficients. However, higher-order fits are not justified. We found cubic fits to be unreliable in that they were sensitive to inclusion or exclusion of single stations. The coefficients of the quadratic fits are given in Table 1.

The quadratic fits for each month are plotted in Fig. 9. The snow accumulates rapidly in the autumn north of Canada and Greenland, but then during winter the Alaskan and Siberian sectors catch up, so that in February the depth is rather uniform across the Arctic at 30 cm. In spring the snow accumulation resumes north of Canada and Greenland, so that the geographical pattern for May resembles that for November. The regional differences are greatest in June, as the snow declines rapidly from May to June north of Alaska and Siberia while it is still accumulating at the higher latitudes near Greenland. This regional variation during June is also seen in surface temperatures derived from satellite measurements in the thermal infrared: above freezing in the Beaufort Sea but still below freezing at higher latitudes [plate 1 of Comiso and Kwok (1996)]. In July the snow is melting everywhere. Snow is usually absent during the second half of July and all of August. The small values in the August map are averages of many zeros together with a few summer snowfall events.

Although the individual measurements show large scatter about the smooth quadratic fit (ε in Table 1), the

TABLE 1. Coefficients for the two-dimensional quadratic fit to snow depth. A rectangular grid is defined with origin at the North Pole, positive x axis along 0°, positive y axis along 90°E. Units of x and y are degrees of arc. Snow depth H (cm) is given by $H = H_0 + Ax + By + Cxy + Dx^2 + Ey^2$, where H_0 is the fitted snow depth at the North Pole. The rms error of the fit (in cm) is given as ε. Also given are the slopes F of the trend lines (Fig. 18) in cm yr^{-1}, and their uncertainty (σ_F). Interannual variability (IAV) is the std dev of the snow depth anomalies (e.g., of the points in Fig. 17).

Month	H_0	A	B	C	D	E	ε	F	σ_F	IAV
Aug	4.64	0.3100	−0.6350	−0.0655	0.0059	−0.0005	4.6	−0.01	0.05	3.3
Sept	15.81	0.2119	−1.0292	−0.0868	−0.0177	−0.0723	7.8	−0.03	0.06	3.8
Oct	22.66	0.3594	−1.3483	−0.1063	0.0051	−0.0577	8.0	−0.08	0.06	4.0
Nov	25.57	0.1496	−1.4643	−0.1409	−0.0079	−0.0258	7.9	−0.05	0.07	4.3
Dec	26.67	−0.1876	−1.4229	−0.1413	−0.0316	−0.0029	8.2	−0.06	0.07	4.8
Jan	28.01	0.1270	−1.1833	−0.1164	−0.0051	0.0243	7.6	−0.06	0.07	4.6
Feb	30.28	0.1056	−0.5908	−0.0263	−0.0049	0.0044	7.9	−0.06	0.08	5.5
Mar	33.89	0.5486	−0.1996	0.0280	0.0216	−0.0176	9.4	−0.04	0.10	6.2
Apr	36.80	0.4046	−0.4005	0.0256	0.0024	−0.0641	9.4	−0.09	0.09	6.1
May	36.93	0.0214	−1.1795	−0.1076	−0.0244	−0.0142	10.6	−0.21	0.09	6.3
Jun	36.59	0.7021	−1.4819	−0.1195	−0.0009	−0.0603	14.1	−0.16	0.12	8.1
Jul	11.02	0.3008	−1.2591	−0.0811	−0.0043	−0.0959	9.5	0.02	0.10	6.7

similarity of the patterns from one month to the next, as well as the steady gradual evolution of the patterns, argues for their validity.

These snow depth values apply only to the snow on multiyear ice and on ice that formed in refreezing leads in early autumn before much snow had fallen. Snow depth is less on new ice that forms in leads opening during winter within the multiyear ice pack; such new ice occupies about 1% of the area of the central Arctic during the 9 months September–May [Fig. 13 of Thorndike et al. (1975)]. However, the snow depth on the new ice rapidly catches up because drifting snow accumulates on the lower-lying surface of the new ice. Figure 1 of Loshchilov (1964) shows the accumulation of snow on young ice that formed in January, when the multiyear ice already had 28 cm of snow. Three months later the snow depths at the two locations were equal. Loshchilov's result may apply only to narrow regions of thin ice bounded by thick ice; data are not available to do a thorough study of this question.

Ice in the marginal seas does not form until October or November, after the heavy snowfalls of September, so the snow depth is less in all seasons. Measurements made on some 500-m lines, 100–300 km from the Siberian coast, were analyzed by Radionov et al. (1996, section 6b). They obtained the average snow depth on ice in these marginal seas as 7 cm at the beginning of winter, 16 cm in January, and 23 cm in April and May.

In all months the greatest snow depth is north of Greenland. This may partly be the result of collection of drift snow by the numerous well-developed pressure ridges in this area, as discussed by Radionov et al. (1996) and also observed by Hanson (1980) in the Beaufort Sea.

These geographical patterns are also borne out by the calculations of moisture transport in the atmosphere by Overland and Turet (1994).

b. Snow density and snow water equivalent

Two-dimensional quadratic functions were also fitted to the snow density measurements for each month. Figure 10 shows the snow density for May, the month of maximum snow depth. The density exhibits little geographical variation across the Arctic. However, it does vary seasonally. The average snow density for the Arctic Ocean (Fig. 11) is only 250 kg m^{-3} in September but increases with settling and wind packing during autumn and winter to 320 kg m^{-3} in May. The highest density is that of the residual melting snow in July. Similar snow densities are found on Antarctic sea ice (Sturm et al. 1998; Jeffries et al. 1997; Massom et al. 1998).

The snow water equivalent (SWE) was usually computed by personnel at each station by multiplying the snow depth and density they measured simultaneously on a snow line, and is given in the station's dataset. If SWE was not given, we converted the snow depth to SWE using the measured density for that date if available. If density was not available for that date, we used the Arctic-mean density for that month from Fig. 11. If density was measured for part of the same year at the station, an offset was computed from the Arctic Ocean–mean density to be used for that station. We plotted the time series of SWE for each station and made choices as in Fig. 8 and then performed two-dimensional quadratic fits just as for snow depth. These are shown in Fig. 12; the coefficients are listed in Table 2. At the peak of the seasonal cycle, the Arctic Ocean average SWE is 11.0 g cm^{-2} (or 11 cm of liquid-equivalent depth).

c. Comparisons to precipitation estimates

The average SWE of 11.0 g cm^{-2} observed on multiyear ice in mid-May (Fig. 12) represents 9 months of solid precipitation (the sum of snowfall, frost deposition and rime deposition, minus sublimation), minus an unknown quantity of snowfall that was lost by drifting into leads and melting there. According to an analysis of meteorological data from the NP drifting stations by Lindsay (1998, Fig. 7), winter sublimation is exceeded by frost deposition; during the 7 months October–April

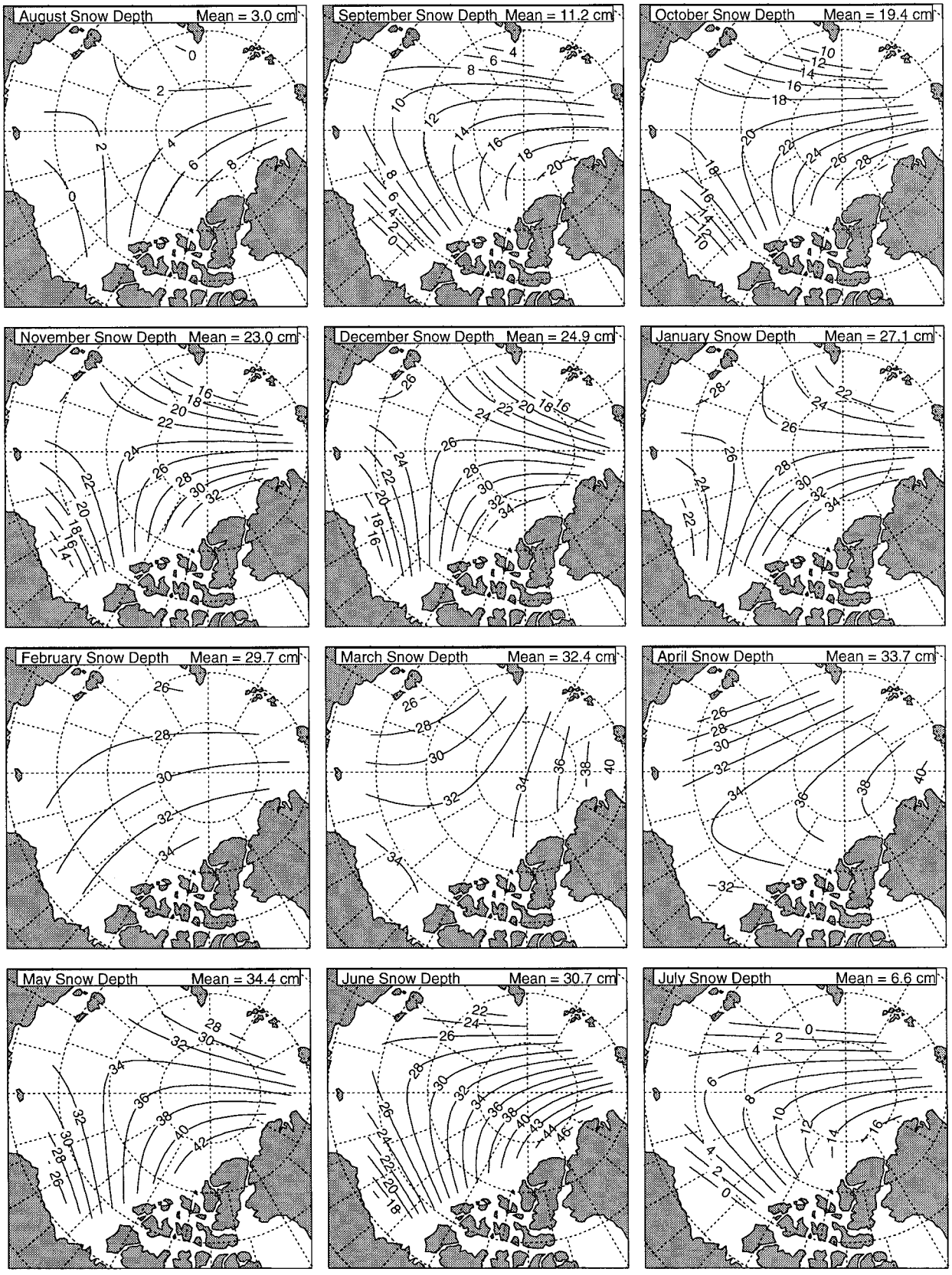

FIG. 9. Mean snow depth for 1954–91 on multiyear sea ice at drifting stations for each month, in cm of geometric depth. A two-dimensional quadratic function was fitted to all the data available for each month, irrespective of year. Coefficients for the fits are given in Table 1.

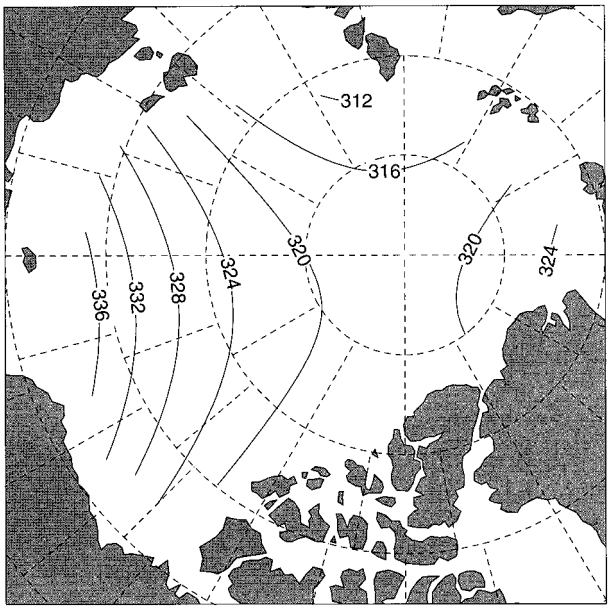

FIG. 10. Mean snow density for the month of May, in kg m^{-3}. A two-dimensional quadratic function was fitted to all the available data for May, irrespective of year (1954–91).

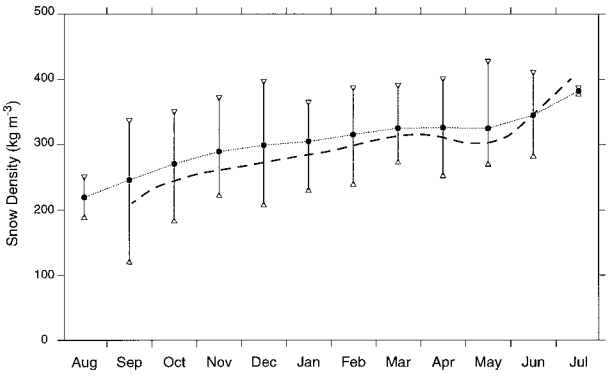

FIG. 11. Multiyear (1954–91) mean snow density for each month (large solid dots). All available density measurements for each month are used, irrespective of year and geographical location. Error bars indicate one standard deviation. Values of Loshchilov (1964) based on measurements at stations NP-2 through NP-9 are shown for comparison as the dashed line.

a net deposition of frost is estimated to contribute 0.5 g cm^{-2}; which is, 5% of the total snow accumulation. [Improved estimates of the winter sublimation might be obtained by applying models of blowing snow, such as those of Pomeroy et al. (1997) and Liston and Sturm (1998).]

Colony et al.'s (1997) analysis of precipitation measurements from the NP stations (their Fig. 3) shows for the 9 months mid-August to mid-May a total of 9.3 g cm^{-2} of snowfall (and 0.6 g cm^{-2} of rain in August–September), implying that the precipitation gauges underestimated the snow precipitation by about 20%. Such discrepancies have often been found when comparing snow accumulation to measured precipitation, particularly at windy locations. Colony et al. estimated a total precipitation (liquid plus solid) of 4.8 g cm^{-2} for the three summer months mid-May to mid-August. Summer precipitation measurements may be more accurate because a larger fraction of the precipitation is rain. If we just add the summer precipitation (4.8) and August–September rain (0.6) to the September–May accumulation (11.0), we obtain 16.4 g cm^{-2} of annual precipitation. This value is surprisingly similar to the average annual precipitation of 18.4 g cm^{-2} estimated for Antarctica (Giovinetto et al. 1992).

In the summer there is significant evaporation. Estimates made by Badgley (1966), Maykut and Untersteiner (1971), Radionov et al. (1996), and Lindsay (1998) are listed in Table 3. The values of Maykut and Untersteiner (1971) were also used by Maykut (1982); they are based on those of Fletcher (1965). The values of Lindsay (1998) were derived from daily atmospheric measurements at the NP drifting stations, so we take them to be the most reliable.

Subtracting Lindsay's summer evaporation (E) of 3.4 g cm^{-2} from the annual precipitation (P), we obtain $P - E = 13$ g cm^{-2} yr^{-1}. This estimate of $P - E$ can be compared to the transport of water vapor through the atmosphere. A network of radiosonde stations surrounding the Arctic was used by Peixoto and Oort (1992, p. 305) to determine the flux of water vapor into the Arctic. A net convergence of 11.7 g cm^{-2} yr^{-1} was estimated for the area north of 70°N for the years 1963–73. Their estimate was updated by Overland and Turet (1994), who obtained 14.3 g cm^{-2} yr^{-1} for the 25 yr 1965–89. A similar analysis by Serreze et al. (1995a) for the 20-yr period 1971–91 obtained 16.3 g cm^{-2} yr^{-1}. Our estimated 13 g cm^{-2} yr^{-1} for $P - E$ at the drifting stations is within the range of these estimates. Exact agreement cannot be expected because the multiyear ice occupies only half of the area north of 70°N.

d. Annual cycles of snow depth

Figures 13 and 14 show annual cycles of snow depth and SWE. The ''Arctic Ocean mean'' is just an average of all the complete annual cycles (August–July) measured at the NP stations. The beginning and ending snow depth years of a station are often not included because their annual cycles are incomplete. There is a rapid accumulation of snow in autumn, very little accumulation in December and January, then a slow steady increase of depth in spring to a maximum in May. This pattern was shown earlier by Untersteiner (1961) and Hanson (1980) in the Beaufort Sea. Hanson measured accumulation of 5 cm SWE $month^{-1}$ in September–October, 1 cm $month^{-1}$ in November–March, and 2 cm $month^{-1}$ in April. September is always found to be the month of greatest snowfall, corresponding to the maximum con-

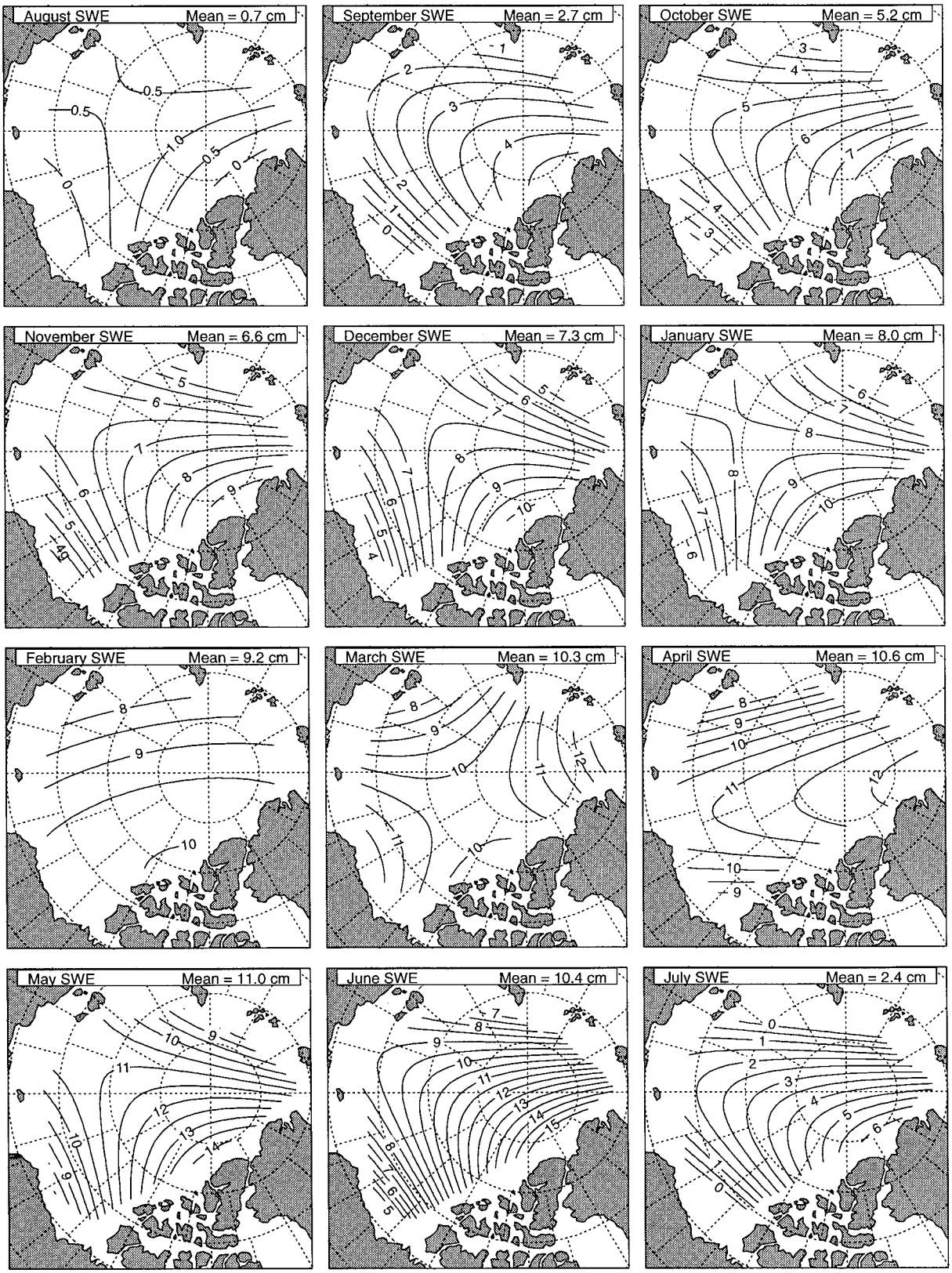

FIG. 12. Mean snow water equivalent (SWE) for 1954–91 on multiyear ice at drifting stations for each month, in cm of liquid equivalent depth. A 2D quadratic function was fitted to all the data available for each month, irrespective of year. Coefficients for the fits are given in Table 2.

TABLE 2. Same as Table 1 but for snow water equivalent

Month	H_0	A	B	C	D	E	ε	F	σ_F	IAV
August	1.08	0.0712	−0.1450	−0.0155	0.0014	−0.0000	1.1	−0.001	0.012	0.8
September	3.84	0.0393	−0.2107	−0.0182	−0.0053	−0.0190	2.0	−0.003	0.016	1.0
October	6.24	0.1158	−0.2803	−0.0215	0.0015	−0.0176	2.3	−0.005	0.021	1.4
November	7.54	0.0567	−0.3201	−0.0284	−0.0032	−0.0129	2.4	−0.000	0.023	1.5
December	8.00	−0.0540	−0.3650	−0.0362	−0.0112	−0.0035	2.5	−0.003	0.024	1.5
January	8.37	−0.0270	−0.3400	−0.0319	−0.0056	−0.0005	2.5	−0.005	0.024	1.6
February	9.43	0.0058	−0.1309	0.0017	−0.0021	−0.0072	2.6	−0.007	0.028	1.8
March	10.74	0.1618	0.0276	0.0213	0.0076	−0.0125	3.1	0.007	0.032	2.1
April	11.67	0.0841	−0.1328	0.0081	−0.0003	−0.0301	3.2	−0.013	0.032	2.1
May	11.80	−0.0043	−0.4284	−0.0380	−0.0071	−0.0063	3.5	−0.047	0.033	2.2
June	12.48	0.2084	−0.5739	−0.0468	−0.0023	−0.0253	4.9	−0.030	0.044	2.9
July	4.01	0.0970	−0.4930	−0.0333	−0.0026	−0.0343	3.5	0.008	0.037	2.4

vergence of atmospheric water vapor in that month [Fig. 4 of Serreze et al. (1995a)].

The melting of Arctic snow cover at a particular location in a particular year often occurs more rapidly than over the full month (mid-June to mid-July) shown in Fig. 13. But in different years the melting occurs at different times during this period, so the multiyear average shows this less rapid decline that is rarely observed in individual years.

The other curves in Fig. 13 are values for three particular locations in the Arctic with contrasting seasonal cycles, the values for each month taken from the contour plots in Fig. 9. The cycle in the Chukchi Sea at 75°N, 180° is similar to that of the Arctic Ocean mean. At 85°N, 90°W near Ellesmere Island the Arctic-mean pattern just described is exaggerated, with no net accumulation at all from December to March, and a substantial increase in spring that is not seen elsewhere. Finally, north of Siberia at 85°N, 90°E there is a rather steady rate of accumulation through the autumn and winter. The corresponding plots for SWE are shown in Fig. 14.

Figure 15 compares our Arctic-mean seasonal cycle to two earlier published records. The record for drifting station A (Untersteiner 1961) is for a single seasonal cycle at a single station, showing the typically rapid snowmelt seen at individual sites as mentioned earlier. The curve from Loshchilov (1964) is a direct predecessor to our work; he analyzed the data for NP stations 2–9. Loshchilov's seasonal cycle was reproduced in Vowinckel and Orvig's (1970) review article, so it is probably the one most used by climate modelers to date. Our climatology updates that of Loshchilov with an additional 28 yr of data. There are a few other measurements of snow depth from non-Soviet drifting stations and ship-based ice camps (Hanson 1965; Maykut and Perovich 1985), but none with full seasonal cycles that can be compared with the analyses here. However, the full year of snow depth measurements in the Beaufort Sea from the experiment on Surface Heat and Energy Balance of the Arctic (Randall et al. 1998) should soon be available for comparison with our maps.

e. Local variations in snow depth: Sastrugi, ridges, and hummocks

The snow line measurements at the NP stations did not explicitly relate snow depth to microtopography. This was, however, attempted by Romanov (1996) at his aircraft landing sites. He distinguished three types of microtopography. Sastrugi are erosional features that align with the wind direction; they can form on a level ice surface. Ridges are formed when neighboring ice floes converge and collide. Hummocks are rounded ice bumps, the eroded remnants of old ridges.

Most of the landings occurred in April. Figure 16 shows the result of fitting two-dimensional quadratics to Romanov's snow depth distributions for April. Because the geographical sampling of the landings was very uneven (concentrating on the coastal shipping route), we first averaged all data within the grid boxes defined in Fig. 3 and then fitted quadratic functions to these grid-box averages. The average snow depths are higher in sastrugi (23 cm) and behind pressure ridges

TABLE 3. Estimates of evaporation from the Arctic Ocean (g cm^{-2}). Conversion from latent heat flux to mass flux was done using the latent heat of sublimation for May and Sep and the latent heat of evaporation for Jun–Aug.

Author	May	June	July	August	September	Total
Badgley (1966)	0.63	0.93	0.50	0.07	0.32	2.45
Maykut and Untersteiner (1971)	0.68	1.17	1.07	1.10	0.57	4.59
Radionov et al. (1996)						
Method a	0.57	1.01	0.92	0.57	0.41	3.48
Method b	0.9	1.3	1.0	0.3	0.4	3.9
Method c	0.8	1.4	1.1	0.7	0.3	4.3
Lindsay (1998)	0.60	1.06	0.67	0.69	0.35	3.37

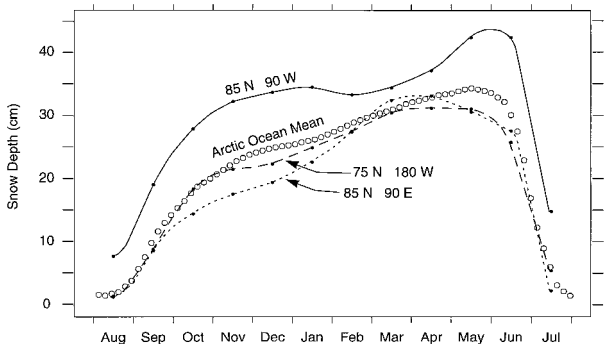

FIG. 13. Seasonal cycles of snow depth on multiyear Arctic sea ice. The mean of all NP stations that sampled complete years (Aug–Jul) is shown, as well as the seasonal cycles at three locations (values taken from Fig. 9).

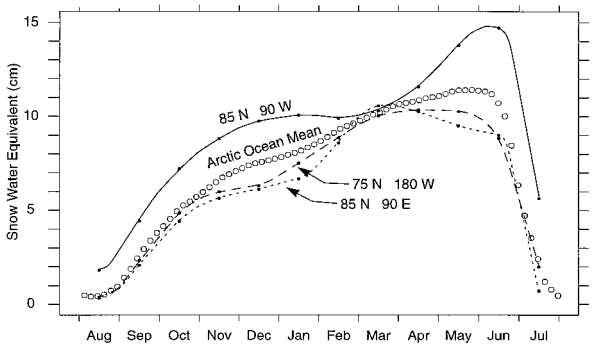

FIG. 14. Same as Fig. 13 but for snow water equivalent.

(22 cm) than on the ice of the landing area (16 cm) as expected, but it is puzzling that the snow should be so much deeper around hummocks (45 cm) than behind ridges.

The geographical patterns are also puzzling. Because some of the variation in average snow depth across the Arctic seen in Fig. 9 is probably due to different areal coverages of sastrugi, ridges, and hummocks, one would expect the geographical gradients of snow *within* these classifications to be smaller than those of Fig. 9. However, this is not the case. The snow depth behind ridges appears to decrease toward Canada, while the height of snow around hummocks increases. These strange patterns cause us to question the representativeness of the measurements made at the aircraft landing sites. We favor the measurements made at the NP stations that were conducted more systematically; they are used exclusively everywhere in this paper except for this one figure.

f. Interannual variations and trends

We define the ''anomaly'' of snow depth in a particular month of a particular year as the snow depth measured at the NP station operating in that year, minus the multiyear average snow depth for the latitude and longitude of the station (which can be obtained from the contour plots in Fig. 9). If only one NP station was reporting, we allow its anomaly to represent the entire Arctic for that month. If more than one station was operating in that year their anomalies are averaged. The anomalies for May, the month of maximum snow depth, are plotted in Fig. 17, together with the least squares trend line. The trend for May is -0.2 cm yr^{-1}.

Our only estimate of the interannual variability (IAV) of the Arctic Ocean mean is the standard deviation of these anomalies. For May it is 6.3 cm. However, it should be noted that this value exceeds the true IAV because it is obtained from measurements at only a few (typically 2) locations so is to some extent recording regional anomalies that are accompanied by unsampled anomalies of opposite sign in other regions in the same month.

Plots like Fig. 17 were made for all months. The IAVs, slopes of trend lines, and uncertainties in the slopes are all given in Table 1. The corresponding values for SWE are given in Table 2. The slopes of the trend lines, together with their uncertainties, are shown in Fig. 18. The trend is significant at the 2σ level only for the month of May, but a decrease in snow depth from 1954 to 1991 is seen in all months except July. The trends are largest in the months of deepest snow.

The decline of snow depth in all months but July may be explained by a decline in winter precipitation. Analysis of the precipitation measurements at the NP stations by Radionov et al. (1996) indeed shows trends from 1954 to 1991 of -0.5 mm SWE yr^{-1} for September–June precipitation and $+0.2$ mm SWE yr^{-1} for July–August precipitation. The trend in annual precipitation is therefore negative. Serreze et al. (1995b) found no significant trend in annual import of atmospheric water vapor during the 17 years 1974–91, but again it applies to the entire latitude zone 70°–90°N, only half of which is occupied by the multiyear ice. The large decline in snow depth in the month of May might also partly be explained by an earlier onset of melting due to climatic warming. Analysis of trends in surface air temperatures

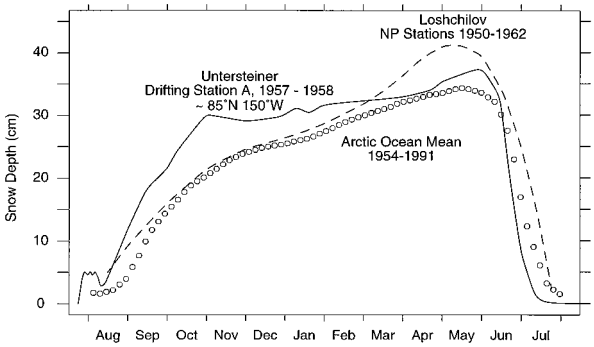

FIG. 15. Mean seasonal cycle of snow depth on multiyear Arctic sea ice (from Fig. 13), compared to earlier published reports using smaller datasets.

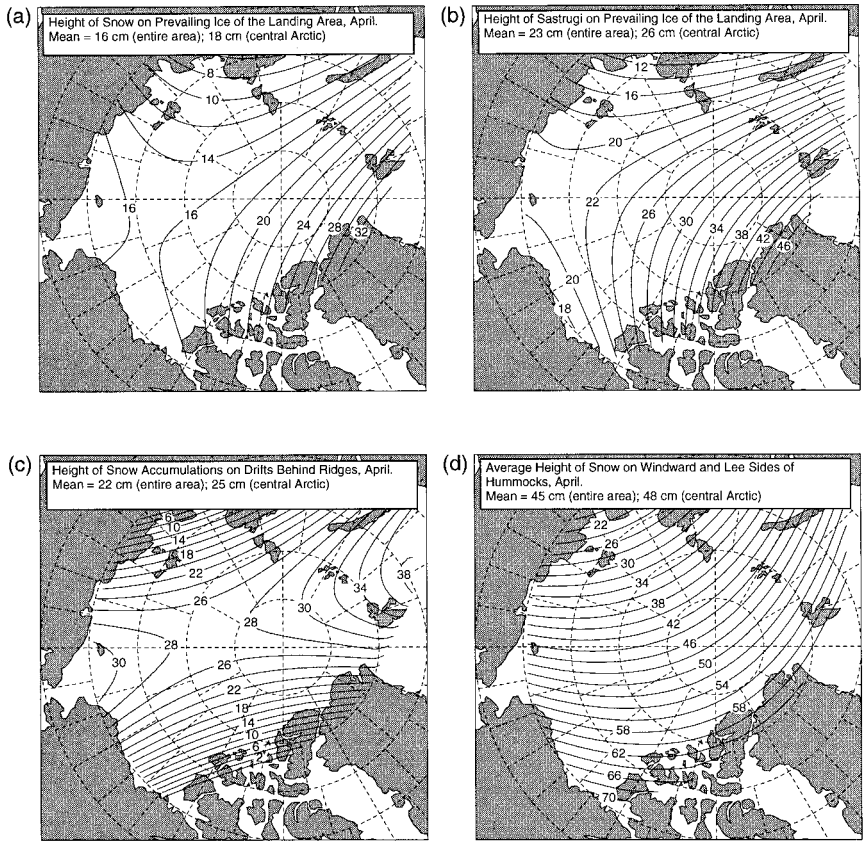

FIG. 16. Snow depth measured at aircraft landing sites of the Sever program (Romanov 1996) in Apr, the month with the most measurements. Average depth is given for snow (a) on the prevailing ice type of the landing area, (b) in sastrugi, (c) in drifts behind ridges, and (d) on the sides of hummocks. The region of the Arctic covered by the aircraft landings (''entire area'') is greater than that covered by the drifting stations (''central Arctic''); mean snow depth for each is given in the legends.

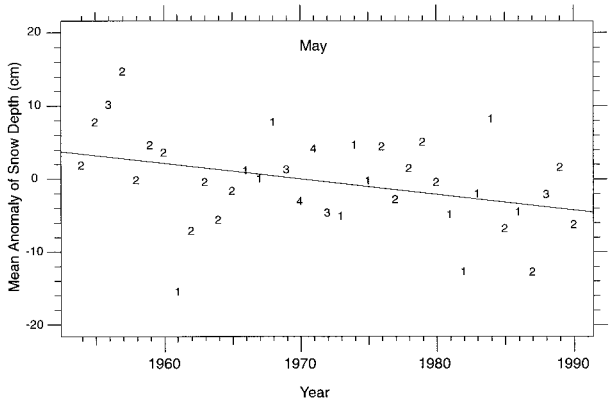

FIG. 17. Interannual variation of snow depth in May, the month of greatest depth. For each year, the snow depth measured at a drifting station in May was compared to the value in Fig. 9 for the location of the station on the day of measurement. The ''anomaly'' is the value for a particular May, minus the multiyear average for May at that location. Each plotted point is the average of the anomalies for all the drifting stations reporting in that year. The digit plotted is the number of stations. The line is a least squares fit to the points.

measured at the NP stations (Martin et al. 1997) shows no significant trend on annual average but a large warming in the month of May (0.08 K yr^{-1}) for the 30 yr 1961–90. However, only one of the 73 spring seasons recorded at the NP stations (NP-28, 1987) shows any indication of snowmelt beginning before June. We therefore cannot attribute the decline in May's snow depth to earlier onset of melt; it must instead be due to reduced snowfall.

We have not identified a cause for the decreasing trend of snowfall. Passive microwave observations of the Arctic Ocean over the period 1979–96, which can distinguish cold snow from water and wet snow (Smith 1998), indicate that the date of freeze-up in early September has been delayed in recent years. If a greater fraction of the September precipitation now falls as rain rather than snow, this could explain part of the reduced snow accumulation. However, reduced contributions to the seasonal snowfall also occur in October, April, and May, as shown in Fig. 18. The decline in snow accumulation may be related in some (as yet undetermined) way to the ''Arctic Oscillation index'' of sea level pressure dif-

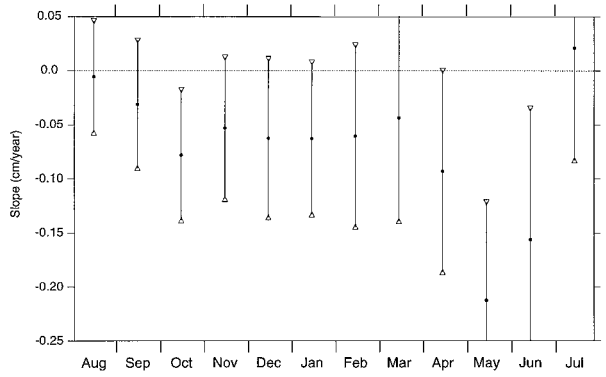

FIG. 18. Slopes of trend lines fitted to interannual anomalies of snow depth from 1954 to 1991, such as that shown for May in Fig. 17. The error bars indicate one std dev.

ferences between the Arctic and the neighboring North Atlantic and North Pacific (Thompson and Wallace 1998). This index was steady from 1900 to 1970 but then increased during 1970–1990, corresponding to a decline in sea level pressure in the central Arctic (Walsh et al. 1996).

4. Conclusions

Systematic measurements of snow depth and density over 37 yr at the Soviet drifting stations have provided the most comprehensive dataset of Arctic Ocean snow cover now available for climatic studies. The last station, NP-31, was decommissioned in 1991, so data of this type are no longer being collected. Satellite remote sensing can be used for subsequent years to monitor the date of disappearance of snow (e.g., Robinson et al. 1992), but there is no remote-sensing method that can infer snow depth accurately during the accumulation season. The continuous climatic record of accurate basic measurements, obtained by numerous dedicated scientists and technicians over many years, is a valuable legacy of the Soviet Union's consistent commitment to meteorological data collection and monitoring of the Arctic environment.

Acknowledgments. The data from drifting stations were made available by a project of the U.S.–Russian Commission on Environmental Cooperation (Gore–Chernomyrdin Commission), with partial funding from the Office of Naval Research. This work was supported by NASA's Polar Research Program Office under Grant NAGW-4382, which also funded the acquisition of the Sever snow depth data. We thank Roger Barry, Chris Bretherton, Thomas Grenfell, Glen Liston, Seelye Martin, Gary Maykut, Il'ya Romanov, Axel Schweiger, and Harry Stern for helpful discussion. SGW acknowledges the hospitality of the Antarctic Cooperative Research Centre at the University of Tasmania during the writing of this paper.

REFERENCES

Badgley, F. I., 1966: Heat budget at the surface of the Arctic Ocean. *Proc. Symp. on the Arctic Heat Budget and Atmospheric Circulation*, Lake Arrowhead, CA, The Rand Corporation, 267–277.

Colony, R., V. Radionov, and F. J. Tanis, 1998: Measurements of precipitation and snow pack at Russian North Pole drifting stations. *Polar Rec.*, **34,** 3–14.

Comiso, J. C., and R. Kwok, 1996: Surface and radiative characteristics of the summer Arctic sea ice cover from multisensor satellite observations. *J. Geophys. Res.*, **101,** 28 397–28 416.

Crary, A. P., 1956: Arctic ice island research. *Advances in Geophysics*, Vol. 3, Academic Press, 1–41.

Fletcher, J. O., 1965: The heat budget of the Arctic Basin and its relation to climate. Rand Rep. R-444-PR, The Rand Corporation, Santa Monica, CA, 179 pp. [Available from Rand Corporation, 1700 Main St., Santa Monica, CA 90406.]

Giovinetto, M. B., D. H. Bromwich, and G. Wendler, 1992: Atmospheric net transport of water vapor and latent heat across 70°S. *J. Geophys. Res.*, **97,** 917–930.

Gloersen, P., W. J. Campbell, D. J. Cavalieri, J. C. Comiso, C. L. Parkinson, and H. J. Zwally, 1992: Arctic and Antarctic sea ice, 1978–1987: Satellite passive-microwave observations and analysis. NASA SP-511, National Aeronautics and Space Administration, Washington, DC, 290 pp. [Available from Scientific and Technical Information Program, NASA, Washington, DC 20024.]

Grenfell, T. C., and G. A. Maykut, 1977: The optical properties of ice and snow in the Arctic Basin. *J. Glaciol.*, **18,** 445–463.

Hanson, A. M., 1965: Studies of the mass budget of arctic pack-ice floes. *J. Glaciol.*, **5,** 701–709.

——, 1980: The snow cover of sea ice during the Arctic Ice Dynamics Joint Experiment, 1975 to 1976. *Arct. Alp. Res.*, **12,** 215–226.

Jeffries, M. O., A. P. Worby, K. Morris, and W. F. Weeks, 1997: Seasonal variations in the properties and structural composition of sea ice and snow cover in the Bellingshausen and Amundsen Seas, Antarctica. *J. Glaciol.*, **43,** 138–151.

Kahl, J. D., M. C. Serreze, S. Shiotani, S. M. Skony, and R. C. Schnell, 1992: In situ meteorological sounding archives for Arctic studies. *Bull. Amer. Meteor. Soc.*, **73,** 1824–1830.

Ledley, T. S., 1991: Snow on sea ice: Competing effects in shaping climate. *J. Geophys. Res.*, **96,** 17 195–17 208.

Lindsay, R. W., 1998: Temporal variability of the energy balance of thick arctic pack ice. *J. Climate*, **11,** 313–333.

Liston, G. E., and M. Sturm, 1998: A snow-transport model for complex terrain. *J. Glaciol.*, **44,** 498–516.

Loshchilov, V. S., 1964: Snow cover on the ice of the central Arctic (in Russian). *Probl. Arct. Antarct.*, **17,** 36–45.

Martin, S., E. Munoz, and R. Drucker, 1997: Recent observations of a spring–summer surface warming over the Arctic Ocean. *Geophys. Res. Lett.*, **24,** 1259–1262.

Massom, R. A., V. I. Lytle, A. P. Worby, and I. Allison, 1998: Winter snow cover variability on East Antarctic sea ice. *J. Geophys. Res.*, **103,** 24 837–24 855.

Maykut, G. A., 1982: Large-scale heat exchange and ice production in the central Arctic. *J. Geophys. Res.*, **87,** 7971–7984.

——, and N. Untersteiner, 1971: Some results from a time-dependent thermodynamic model of sea ice. *J. Geophys. Res.*, **76,** 1550–1575.

——, and D. K. Perovich, 1985: MIZEX 84 heat and mass balance data. Rep. APL-UW 12-85, Applied Physics Laboratory, University of Washington, Seattle, WA, 6–15. [Available from Applied Physics Laboratory, University of Washington, Seattle, WA 98195.]

Overland, J. E., and P. Turet, 1994: Variability of the atmospheric energy flux across 70°N computed from the GFDL data set. *The Polar Oceans and Their Role in Shaping the Global Environment, Geophys. Monogr.*, No. 84, Amer. Geophys. Union, 313–325.

Peixoto, J. P., and A. H. Oort, 1992: *Physics of Climate.* American Institute of Physics, 520 pp.

Pomeroy, J. W., P. Marsh, and D. M. Gray, 1997: Application of a distributed blowing snow model to the Arctic. *Hydrol. Processes,* **11,** 1451–1464.

Radionov, V. F., N. N. Bryazgin, and Ye. I. Aleksandrov, 1996: *The Snow Cover of the Arctic Basin* (in Russian). Gidrometeoizdat, 102 pp. [English translation available from Polar Science Center, University of Washington, Seattle, WA 98195; Tech. Rep. APL-UW TR 9701.]

Randall, D., and Coauthors, 1998: Status of and outlook for large-scale modeling of atmosphere–ice–ocean interactions in the Arctic. *Bull. Amer. Meteor. Soc.,* **79,** 197–219.

Robinson, D. A., M. C. Serreze, R. G. Barry, G. Scharfen, and G. Kukla, 1992: Large-scale patterns and variability of snowmelt and parameterized surface albedo in the Arctic Basin. *J. Climate,* **5,** 1109–1119.

Romanov, I. P., 1996: *Atlas of Ice and Snow of the Arctic Basin and Siberian Shelf Seas.* Backbone Publishing, 211 pp. and 250 charts.

Serreze, M. C., R. G. Barry, and J. E. Walsh, 1995a: Atmospheric water vapor characteristics at 70°N. *J. Climate,* **8,** 719–731.

——, ——, M. C. Rehder, and J. E. Walsh, 1995b: Variability in atmospheric circulation and moisture flux over the Arctic. *Philos. Trans. Roy. Soc. London,* **A352,** 215–225.

Smith, D. M., 1998: Recent increase in the length of the melt season of perennial Arctic sea ice. *Geophys. Res. Lett.,* **25,** 655–658.

Sturm, M., J. Holmgren, M. König, and K. Morris, 1997: The thermal conductivity of seasonal snow. *J. Glaciol.,* **43,** 26–41.

——, K. Morris, and R. Massom, 1998: The winter snow cover of the west Antarctic pack ice: Its spatial and temporal variability. *Antarct. Res. Ser.,* **74,** 1–18.

Thompson, D. W. J., and J. M. Wallace, 1998: The Arctic oscillation signature in the wintertime geopotential height and temperature fields. *Geophys. Res. Lett.,* **25,** 1297–1300.

Thorndike, A. S., D. A. Rothrock, G. A. Maykut, and R. Colony, 1975: The thickness distribution of sea ice. *J. Geophys. Res.,* **80,** 4501–4513.

Untersteiner, N., 1961: On the mass and heat budget of Arctic sea ice. *Arch. Meteor. Geophys. Bioklimatol.,* **A12,** 151–182.

Vowinckel, E., and S. Orvig, 1970: The climate of the north polar basin. *Climates of the Polar Regions, World Survey of Climatology,* S. Orvig, Ed., Vol. 14, Elsevier, 129–252.

Walsh, J. E., W. L. Chapman, and T. L. Shy, 1996: Recent decrease of sea level pressure in the central Arctic. *J. Climate,* **9,** 480–486.